The effect of emission source chemical profiles on simulated $PM_{2.5}$ components: sensitivity analysis with CMAQv5.0.2

Zhongwei Luo[a,b,1], Yan Han[a,b,c,1], Kun Hua[a,b], Yufen Zhang[a,b*], Jianhui Wu[a,b], Xiaohui Bi[a,b], Qili Dai[a,b], Baoshuang Liu[a,b], Yang Chen[c], Xin Long[c], Yinchang Feng[a,b*]

[a]State Environmental Protection Key Laboratory of Urban Ambient Air Particulate Matter Pollution Prevention and Control & Tianjin Key Laboratory of Urban Transport Emission Research, College of Environmental Science and Engineering, Nankai University, Tianjin 300350, China.

[b]CMA-NKU Cooperative Laboratory for Atmospheric Environment-Health Research, Tianjin 300350, China.

[c]Research Center for Atmospheric Environment, Chongqing Institute of Green and Intelligent Technology, Chinese Academy of Sciences, Chongqing 400714, China.

*Corresponding authors:

Y. F. Zhang (zhafox@nankai.edu.cn). And Y. C. Feng (fengyc@nankai.edu.cn).

[1]Z. W. Luo and Y. Han equally contribute to this work

Abstract

The chemical transport model (CTM) is an essential tool for air quality prediction and management, widely used in air pollution control and health risk assessment. However, the current models do not perform very well in reproducing the observations of some major chemical components, for example, sulfate, nitrate, ammonium and organic carbon. Studies suggested that the uncertainties of model chemical mechanism, source emission inventory and meteorological field can cause inaccurate simulation results. Still, the emission source profile (used to create speciated emission inventories for CTMs) of $PM_{2.5}$ has not been fully taken into account in current numerical simulation. Based on the characteristics and variation rules of chemical components in typical $PM_{2.5}$ sources, different simulation scenarios were designed and the sensitivity of simulated $PM_{2.5}$ components to source chemical profile was explored. Our findings showed that the influence of source profile changes on simulated $PM_{2.5}$ components' concentrations could not be ignored. Simulation results of some components were sensitive to the adopted source profile in CTMs. Moreover, there was a linkage effect, the variation of some components in the source profile would bring changes to the simulated results of other components. These influences are connected to chemical mechanisms of the model since the variation of species allocations in emission sources can affect potential composition and phase state of aerosols, chemical reaction priority and multicomponent chemical balance in thermodynamic equilibrium system. We also found that the perturbation of $PM_{2.5}$ source profile caused the variation of simulated gaseous pollutants, which indirectly indicated that the perturbation of source profile would affect the simulation of secondary $PM_{2.5}$ components. Our paper highlights the necessity that the representativeness and timeliness of the source profile should be paid enough attention when using CTMs for simulation.

Keywords

$PM_{2.5}$; source profile; component; numerical simulation; chemical transport model

1. Introduction

Ambient fine particulate matter ($PM_{2.5}$) pollution in some key regions of China has attracted much attention (Liang et al., 2020; Huang et al., 2021). The chemical components of $PM_{2.5}$, including elements (Al, Si, Fe, Mn, Ti, Cu, Zn, Pb, etc.), water-soluble ions (SO_4^{2-}, NO_3^-, Cl^-, F^-, NH_4^+, Na^+, K^+, Mg^{2+}, Ca^{2+}, etc.), and carbon-containing components (Organic Carbon, OC; Elemental Carbon, EC) (Yang et al., 2011; Li et al., 2013), have different physical and chemical properties, such as reactivity, thermal stability, particle size distribution, residence time, optical properties, health hazards, etc (Seinfeld and Pandis, 2006; Tang et al., 2006). According to long-term monitoring results, in most regions of China, SO_4^{2-}, NO_3^-, NH_4^+ and OC are the most important species in ambient $PM_{2.5}$ (Li et al., 2017a; Li et al., 2021), which has a certain adverse impact on human health (Shi et al., 2018) and ecosystem, such as acid rain in southwest China (Han et al., 2019), food security (Zhou et al., 2018), etc.

The chemical transport models (CTMs) play an important role in policy making for regulatory purposes. Based on the scientific understanding of atmospheric physical and chemical processes, CTMs are built to simulate the transport, reaction and removal of pollutants on a certain scale in horizontal and vertical directions. With the development of CTMs, the simulation accuracy of $PM_{2.5}$ concentration has been significantly improved. Higher requirements have been put forward for the precise simulation of $PM_{2.5}$ components so as to provide support for the use of CTMs in human health risk assessment, climate effects, pollution sources apportionment, and so on (Peterson et al., 2020; Lv et al., 2021). However, the current models perform not very well in simulating some components (for example, $PM_{2.5}$-bound sulfate, nitrate, ammonium, trace elements, etc.) (Zheng et al., 2015; Fu et al., 2016; Ying et al., 2018; Cao et al., 2021). In the current literatures, the correlation coefficient (R) and normalized mean bias (NMB) are highly variable and inconsistent between the simulated and the observed values (listed in Table S1). This is mainly attributable to the uncertainties of model chemical mechanism, source emission inventory and

meteorological field simulation.

The chemical mechanisms involved in CTMs are derived from parameterized assumptions based on laboratory simulation and field observations. The actual atmospheric chemical processes are very complex, and some reaction mechanisms are still limitedly understood. In addition, the integration of chemical reactions and simplified treatment methods in the model cannot fully reflect the correlation among atmospheric pollutants. For example, in some model mechanisms, important sulfate and nitrate formation pathways through new heterogeneous chemistry were added, including the chemical reaction between SO_2 and aerosol, $NO_2/NO_3/N_2O_3$ and aerosol (Zheng et al., 2015), nitrous acid oxidized SO_2 to produce sulfate (Zheng et al., 2020), dust particles promoted the oxidation of SO_2 (Yu et al., 2020), modified the uptake coefficients for heterogeneous oxidation of SO_2 to sulfate (Zhang et al., 2019), updated the heterogeneous N_2O_5 parameterization (Foley et al., 2010). Even though the aforementioned processes can significantly improve the simulation of SO_4^{2-} and NO_3^-, there is still a gap between the modeled and the actual atmospheric chemical processes.

The uncertainty of meteorological field simulation is another crucial reason for the simulation deviation, especially on heavy pollution days, the variation trends of $PM_{2.5}$ chemical components were not well-captured (Ying et al., 2018; Qi et al., 2019; Wang et al., 2022). Precipitation is the key meteorological factor determining wet removal of pollutants; boundary layer height and wind speed are the main factors affecting convection and transport of pollutants; solar radiation, temperature and relative humidity are the key factors affecting the formation of secondary particles (Huang et al., 2019; Chen et al., 2020). Some literature reported that deviation from precipitation and wind field simulation might lead to underestimation of SO_4^{2-}, NO_3^- and NH_4^+ (Cheng et al., 2015; Zhang et al., 2017). Devaluation of liquid water path and cloud cover cause a decrease of sulfate formation in cloud, and ultimately results in significantly underestimated components in simulation values (Sha et al., 2019; Foley et al., 2010). Underestimation of temperature and relative humidity may also cause adverse effects of temperature- and/or relative humidity-dependence chemical reaction

in the simulation (Sha et al., 2019).

The uncertainty of source emission inventory also significantly affects the simulation results of $PM_{2.5}$ components (Shi et al., 2017; Sha et al., 2019). Due to incomplete information or insufficient representativeness, pollutant emissions are sometimes overestimated or underestimated, and the method for temporal and spatial allocation also needs to be improved.

In particular, the emission source profile of $PM_{2.5}$ (Hereinafter referred to as "source profile"), used to create speciated emission inventories for CTMs (Hsu et al., 2019), has not been fully taken into account in the current numerical simulation. In the reported literatures, $PM_{2.5}$ species allocation coefficients of emission sources are commonly treated in the following ways: (1) allocated $PM_{2.5}$ components of source emissions by referring to source profile data in published literature or database like the US SPECIATE (Fu et al., 2013; Wang et al., 2014; Ying et al., 2018); (2) chemical profiles come from local measurement (Fu et al., 2013; Appel et al., 2013). However, with the development of production technology and the innovation of pollution treatment technology in recent years, some source profiles have changed dramatically (Bi et al., 2019), such as SO_4^{2-} from coal burning, its content in $PM_{2.5}$ is generally low in coal-fired power plant without desulfurizing facilities, while existing coal-fired power plants using limestone/gypsum wet desulphurization, the contents of SO_4^{2-} in $PM_{2.5}$ are significantly higher than that without desulfurization facilities (Zhang et al., 2020). The timeliness of $PM_{2.5}$ species allocation coefficients in current CTMs also needs to be considered.

This paper attempts to answer the following questions: (1) Whether the variation of the source profile adopted in the model has an impact on the simulated results of $PM_{2.5}$ chemical components? (2) How much does it impact? (3) How does the impact work? Aiming at these problems above, chemical composition and its variation law for typical $PM_{2.5}$ emission sources are summarized, on this basis, sensitivity tests are designed to identify whether $PM_{2.5}$ source profiles and species allocation in the model are important parameters that affect the simulation results of chemical components'

concentrations in $PM_{2.5}$. We take CMAQ (one of the most widely used CTMs), MEIC (a high-resolution inventory of anthropogenic air pollutants in China) as the carriers. The same kind of experiment is also applicable to other CTMs and emission inventories. The aim of this study is to provide support for the effective utilization of source profiles in the CTMs and improvement of the simulation schemes.

2. Model and Data

2.1 Model configuration

Weather Research and Forecasting model (WRF-3.7.1), the widely used Community Multiscale Air Quality model (CMAQv5.0.2) (Eder and Yu, 2006; Yu et al., 2014), and Multi-resolution Emission Inventory for China (MEICv1.3) have been used in this study. MEIC, developed by Tsinghua University, mainly tracked anthropogenic emissions in China including coal-fired power plants, industry, vehicles, residents and agriculture (http://meicmodel.org/?page_id=135) (Li et al., 2017b; Zheng et al., 2018). The WRF model was used to generate meteorological inputs for the CMAQ model. Three nested modeling domains consisting of 36 km×36 km (Dom1), 12 km×12km (Dom2), and 4 km×4km (Dom3) horizontal grid sizes were set, as shown in Fig. 1. The initial and boundary conditions for WRF were based on the North American Regional Reanalysis data archived at National Center for Atmospheric Research (NCAR). In addition, surface and upper air observations obtained from NCAR were used to further refine the analysis data. The modeling was conducted from Oct. 1 to Oct.30 in 2018, and major configurations we used in CMAQ were illuminated as follows: Gas-phase chemistry was based on the CB05 mechanism and the aerosol dynamics/chemistry was based on the aero6 module (cb05tucl_ae6_aq). The detailed model configurations were shown in Table S2, and regional distribution of $PM_{2.5}$ emission sources were shown in Figure S1.

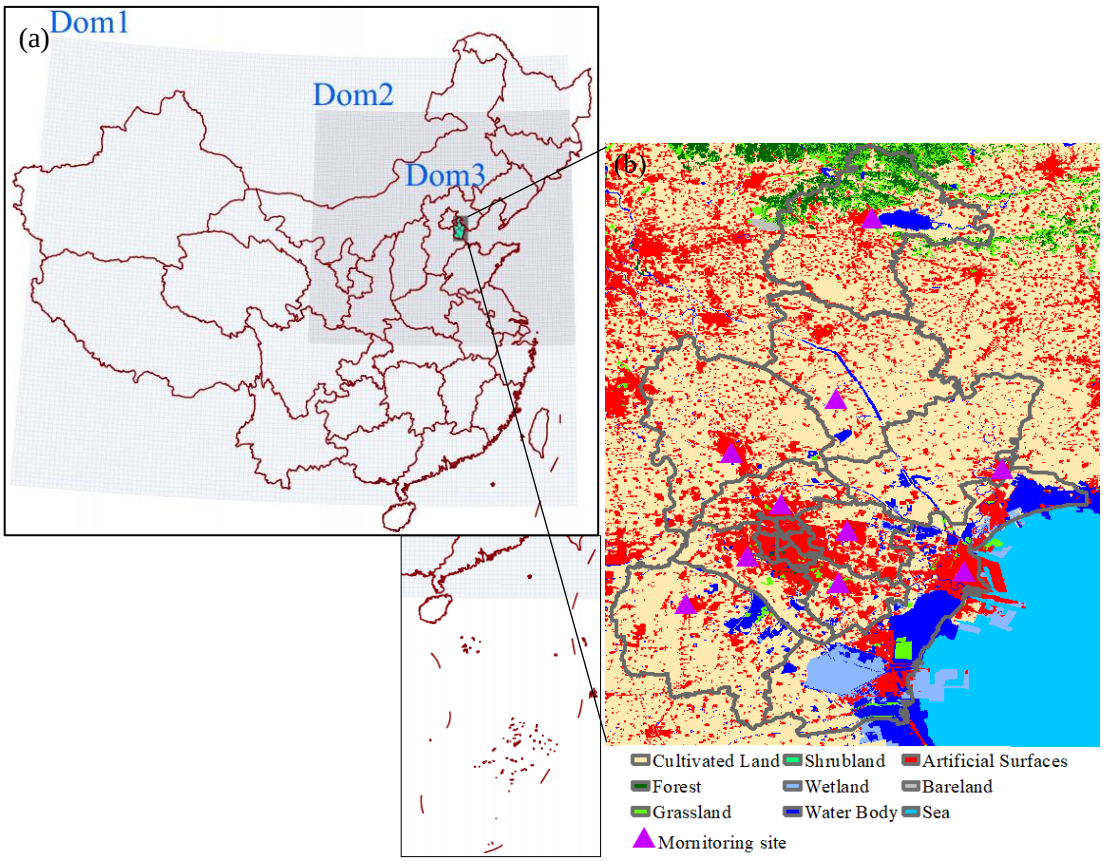

Fig.1 Modeling domains of the CMAQ model. (a) The three-domain nested CMAQ domains; (b) Land use and observation sites of Dom3 (Data source of Land use: GLOBELAND30, www.globeland30.org, National Geomatics Center of China).

2.2 Selection and comparison of $PM_{2.5}$ emission source profile

The $PM_{2.5}$ emission source profiles from database of Source Profiles of Air Pollution (SPAP) (http://www.nkspap.com:9091/), U.S. Environmental Protection Agency's (EPA) SPECIATE database (https://www.epa.gov/air-emissions-modeling/speciate) as well as from published literature were selected, respectively. The SPAP was developed by the State Environment Protection Key Laboratory of Urban Particulate Air Pollution Prevention, Nankai University, China. This database contains more than 3000 size-resolved source profiles of stationary combustion sources, industrial processes, vehicle exhaust, biomass burning, dust and other sources, collected from more than 40 cities in China since 2001. In addition to inorganic elements, water-soluble ions, OC, EC and other conventional components, some source profiles also encompass a series of tracer information, such as organic markers, isotopes, single particle mass spectrometry, VOCs and other gaseous precursors. Based on species in

the aerosol chemical mechanism (AERO6) of CMAQ (Appel et al., 2013; Chapel Hill, 2012), we selected 15 components in $PM_{2.5}$ source profiles including Al, Ca, Cl, EC, Fe, K, Mg, Mn, Na, OC, Si, Ti, NH_4^+, NO_3^- and SO_4^{2-}, the remaining components are classified as "other". In the database of Source Profiles of Air Pollution (SPAP) and U.S. Environmental Protection Agency's (EPA) SPECIATE database, these four source categories (coal-fired power plant, industry process, transportation sector and residential coal combustion) contain a series of sub-categories. But the MEIC emission inventory does not include the corresponding sub-categories. So we take the average values of source profiles in each source category as representing source profile, the details could also be seen in our previous work (Bi et al., 2019); Then multiply inventory emissions by profile fraction to get emissions of specific chemical components.

To determine the similarity between the two groups of source profiles, Coefficient Divergence (CD) is calculated using the following formula (Wongphatarakul et al., 1998):

$$CD_{jk} = \sqrt{\frac{1}{p}\sum_{i=1}^{p}\left(\frac{x_{ij}-x_{ik}}{x_{ij}+x_{ik}}\right)^2} \quad \text{..... (1)}$$

Where CD_{jk} is the coefficient of divergence of source profile j and k, p is the number of chemical components in source profile, x_{ij} is the weight percentage for chemical component i in source profile j, x_{ik} is the weight percentage for i in source profile k (%). The CD value is in the range of 0 to 1, if the two source profiles are similar, the value of CD is close to 0; if the two are very different, the value is close to 1.

Coal-fired power plant (PP)**.** Coal-fired power plants remain the main coal consumers in China, which accounted for 50.2% of total coal consumption in 2019 (NBS, 2021) and gained much more attention, especially with the wide implementation of the ultralow emission standards, $PM_{2.5}$ emission characteristics have changed accordingly (Wu et al., 2020; Wu et al., 2022). There are obvious differences in $PM_{2.5}$ source profiles between SPAPPC (SPAP database and published source profiles in

China) and SPECIATE (U.S.EPA SPECIATE database), the CD value of these two groups lie between 0.34 and 0.92 (0.64±0.10), detailed information is shown in Table S3 and Figure S2. The percentages of species in PP source profiles are plotted in Fig. 2(a). The main components in SPAPPC are sorted by Si, SO_4^{2-}, OC, Ca with average values of 8.7±6.8%, 8.5±11.5%, 6.8±9.1% and 6.5±6.9%, respectively; The SPECIATE are enriched in SO_4^{2-} (16.9%±20.0%), OC (12.7±21.8%), Si (9.6±5.0%) and Ca (9.3±7.3%), higher than SPAPPC. Coal properties, burning conditions, pollution control measures and emission sampling methods are the main reasons for those great percentage fluctuations. Different treatment processes of flue gases, e.g. wet/dry limestone, ammonia and double-alkali flue gas desulfurization, will affect the percentages of components in source profiles (Zhang et al., 2020). It has been reported that the percentage of Ca, Mg, SO_4^{2-} and Cl^- in PP profiles increased after the limestone-gypsum method was used in coal-fired power plants (Bi et al., 2019). Besides that, the percentage of Cl^- in SPAPPC is obviously higher than that in SPECIATE, which might attribute to the generally higher Cl^- content in raw coal in China (Guo et al., 2004).

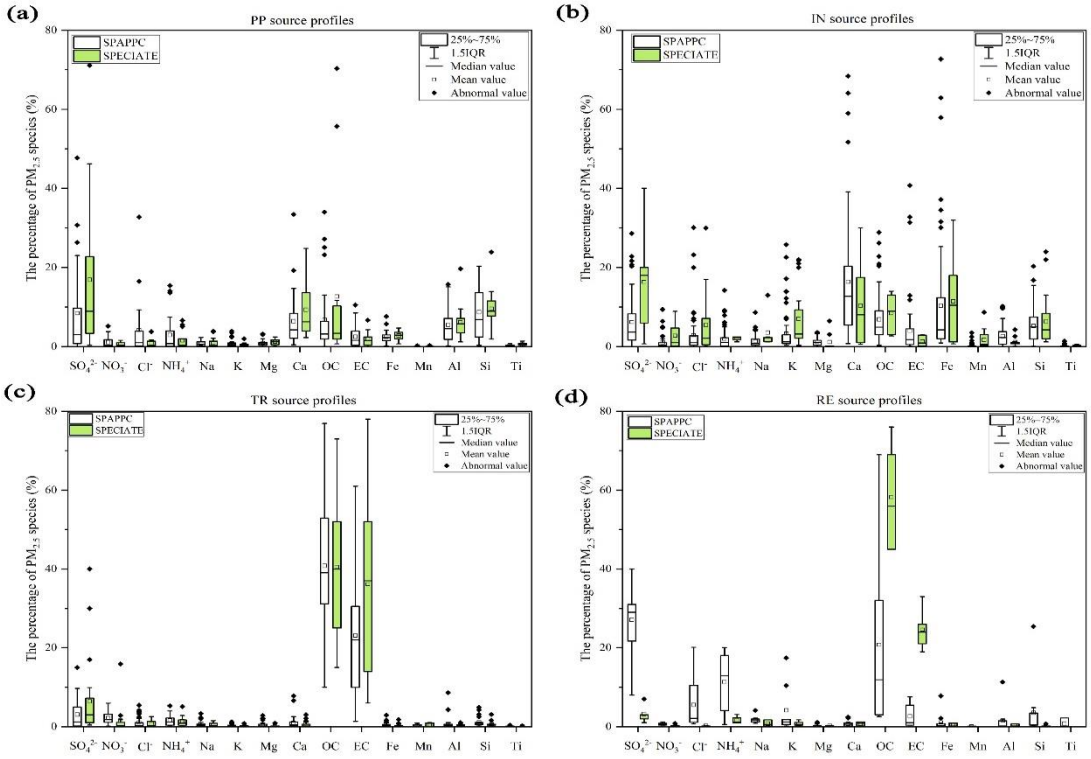

Fig. 2 Chemical profiles for $PM_{2.5}$ emitted from (a) coal-fired power plants (PP), (b) industry processes (IN), (c) transportation sector (TR), (d) residential coal combustion (RE). Data obtained

from SPAPPC (SPAP database and published source profiles in China) and SPECIATE (U.S. EPA SPECIATE database)

Industrial process(IN). Industrial emissions are one of the major sources of $PM_{2.5}$ (Hopke et al., 2020), the percentages of Ca, Fe, OC and SO_4^{2-} are relatively high both in SPAPPC and SPECIATE, but the shares in different source profile database varied, their CD values vary from 0.45 to 0.94 (0.72±0.09) (Detailed information were shown in Table S4~S7 and Figure S3). In SPAPPC, these four components account for 16.4±14.9%, 10.4±14.4%, 6.9±6.1%, 6.2±6.4%, the proportions in SPECIATE are 10.4±9.8%, 11.4±10.6%, 8.5±4.9%, 16.3±13.3%, respectively (Fig. 2(b)). Large variations of components and their percentages in industrial processes are attributed to the manufacturing processes, raw material, pollution control measures and so on (Ji et al., 2017; Bi et al., 2019; Gao et al., 2022). For example, Ca, Al, OC and SO_4^{2-} are found to have the highest percentage in cement sources (Guo et al., 2021); Fe, Si and SO_4^{2-} are the most abundant species in steel industry emission (Guo et al., 2017).

Transportation sector (TR). Traffic contributed a large fraction of $PM_{2.5}$ in many locations (Hopke et al., 2022). It is well-known that the transportation sector makes a dominant contribution of OC and EC. The main components of $PM_{2.5}$ emitted from traffic sources are OC, EC and SO_4^{2-} both in SPAPPC and SPECIATE, but still vary in wide range, their CD values fall between 0.33 and 0.86 (0.69±0.09) (Detailed information was given in Table S8~S10 and Figure S4). In SPAPPC, the percentages of OC, EC and SO_4^{2-} are 40.8±15.0%, 23.1±13.8%, 3.1±3.7%, and in SPECIATE, the percentages are 40.6±16.4%, 36.1±21.5%, 6.4±9.9%, respectively (Fig. 2(c)). These significant differences mainly attribute to the vehicle type, fuel quality, mixing ratio between oil and gas and the combustion phase in vehicle engine and so on (Xia et al., 2017).

Residential coal combustion (RE). Residential coal combustion, as the leading source of global $PM_{2.5}$ emission (Weagle et al., 2018), has a much higher emission factor than coal-fired power plant (Wu et al., 2022). The fraction of components vary greatly in the profiles measured from SPAPPC and SPECIATE, their CD values are 0.75±0.10 (Detailed information was given in Table S11 and Figure S5), SO_4^{2-}, OC,

NH_4^+ and EC make the main contribution to $PM_{2.5}$ emitted from residential coal combustion. In SPAPPC, the average percentages of SO_4^{2-}, OC, NH_4^+, EC are 27.1±10.1%, 20.7±20.6%, 11.3±7.7%, 2.6±2.8%, respectively. In SPECIATE, the average percentages are OC (58.2±14.0%), EC (24.6±5.4%), SO_4^{2-} (3.2±2.3%) and NH_4^+ (1.6±1.0%) (Fig. 2(d)). Total percentages of OC and EC in SPECIATE are over 80%, obviously higher than that in SPAPPC, while a higher percentage of SO_4^{2-}, Cl^-, K and Si are observed in SPAPPC. The coal type and properties, burning condition are the main factors affecting the percentages of $PM_{2.5}$ components, like the chunk coal burning has relatively higher percentages of OC, EC, SO_4^{2-}, NO_3^- and NH_4^+ than honeycomb briquette (Wu et al., 2021; Song et al., 2021).

Briefly, many factors can affect $PM_{2.5}$ source profiles, and with the innovation of manufacturing technique and pollution control technology, changes in fuel and raw and auxiliary materials, the main chemical components and their percentages would change dramatically. To explore whether the variations of source profile adopted in CMAQ model would be one of the important factors affecting the simulated $PM_{2.5}$ component, we designed a series of simulation tests to address the following issues.

3 Is there an impact of variation of source profile on the simulation results?

In this part, we separately selected source profiles from SPAPPC and SPECIATE databases and applied them in emission inventory for simulating $PM_{2.5}$ and its components with other modeling conditions unchanged, corresponding to case CMAQ_SPA and CMAQ_SPE. The detail information of source profiles were shown in Figure S6.

By comparing the selected SPAPPC source profiles with the selected SPECIATE source profiles, the coefficient divergences for the four main source categories were $CD_{PP}(0.67)>CD_{RE}(0.62)>CD_{TR}(0.60)>CD_{IN}(0.60)$, which meant the selected source profiles in the two simulation cases were quite different. The average simulated concentration of $PM_{2.5}$ and its components at each ambient air quality monitoring station (Table S12) were extracted from CMAQ outputs. We selected one air quality

monitoring station (Site 8 as the selected station here and any site could be available) to explore the effect of emission source chemical profiles on simulated $PM_{2.5}$ components, then used the left 9 sites to further illustrate the conclusions suggested.

The simulation results for $PM_{2.5}$ species under CMAQ_SPA and CMAQ_SPE cases also showed big differences (as shown in Fig. 3 and Table S13). The largest difference in average simulated concentration was EC with CAMQ_SPE giving higher by 167% than CMAQ_SPA; For OC and Mn, higher values were also given by CMAQ_SPE than by CMAQ_SPA (45% and 126% on average, respectively); For the other components of concern, the simulated concentration by CMAQ_SPE was lower than CMAQ_SPA with Ti (58%), Na (55%), Mg (53%), Ca (51%), Al (33%), Cl (31%), K (29%), Si (22%), Fe (16%), NH_4^+ (3%), SO_4^{2-} (9%), NO_3^- (8%), separately. While the simulated $PM_{2.5}$ concentrations under the two cases were quite close. The influence of source profile variation on the simulated $PM_{2.5}$ concentration was not significant, but the influence on the simulation of chemical components in $PM_{2.5}$ could not be ignored.

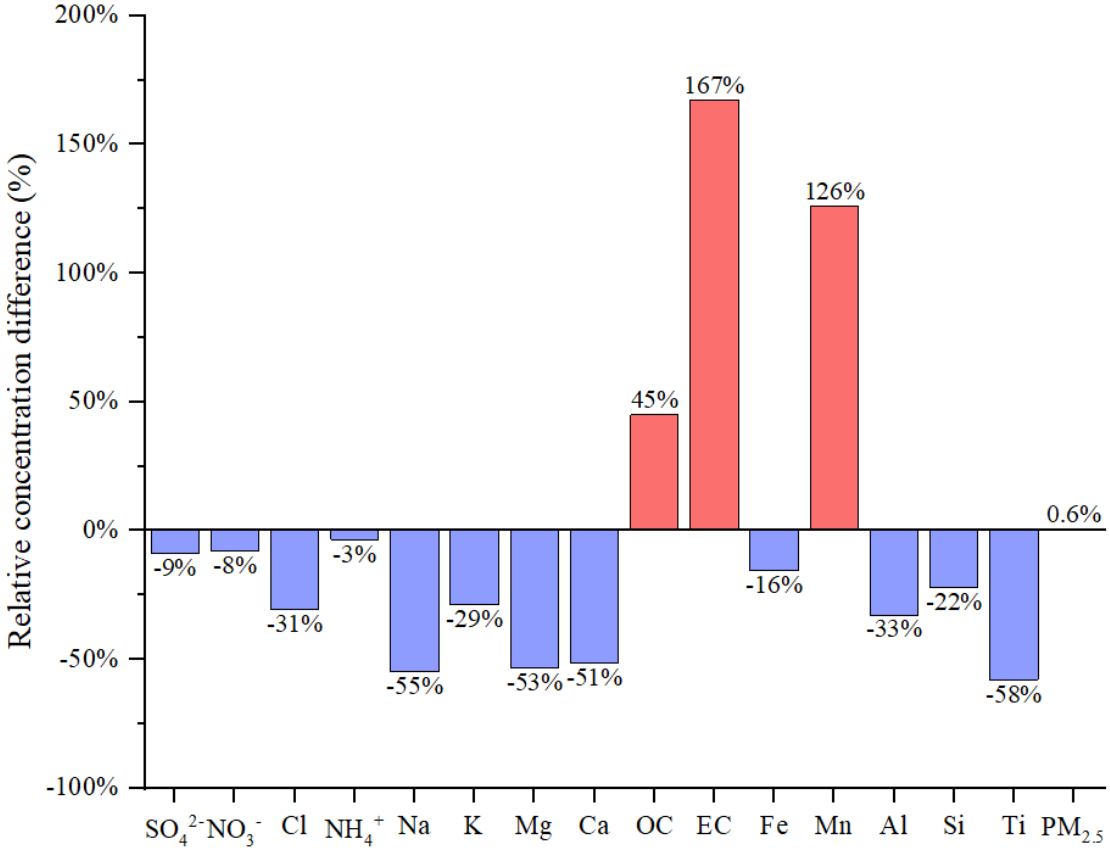

Fig. 3 The relative concentration difference of average simulated results ($PM_{2.5}$ and its components)

between CMAQ_SPE and CAMQ_SPA (relative to CAMQ_SPA) during simulation period; $PM_{2.5}$ source profiles from SPAPPC and SPECIATE database were used to create speciated emission inventories for CMAQ, corresponding to case CMAQ_SPA and CMAQ_SPE, respectively.

4 How much does it impact?

To quantitatively characterize how much the source profiles affect the simulation results, we selected the chemical composition of code 000002.5 (Variety of different categories, used for the overall average composite profiles (Hsu et al., 2019) in the US EPA Speciate_5.0_0 database for species allocation of $PM_{2.5}$ components. The corresponding percentages of EC, OC, Mn, Fe, Ti, Al, Si, Ca, Mg, K, Na, Cl, NH_4^+, NO_3^- and SO_4^{2-} in $PM_{2.5}$ were shown in Fig. 4 (SGL, base case simulation).

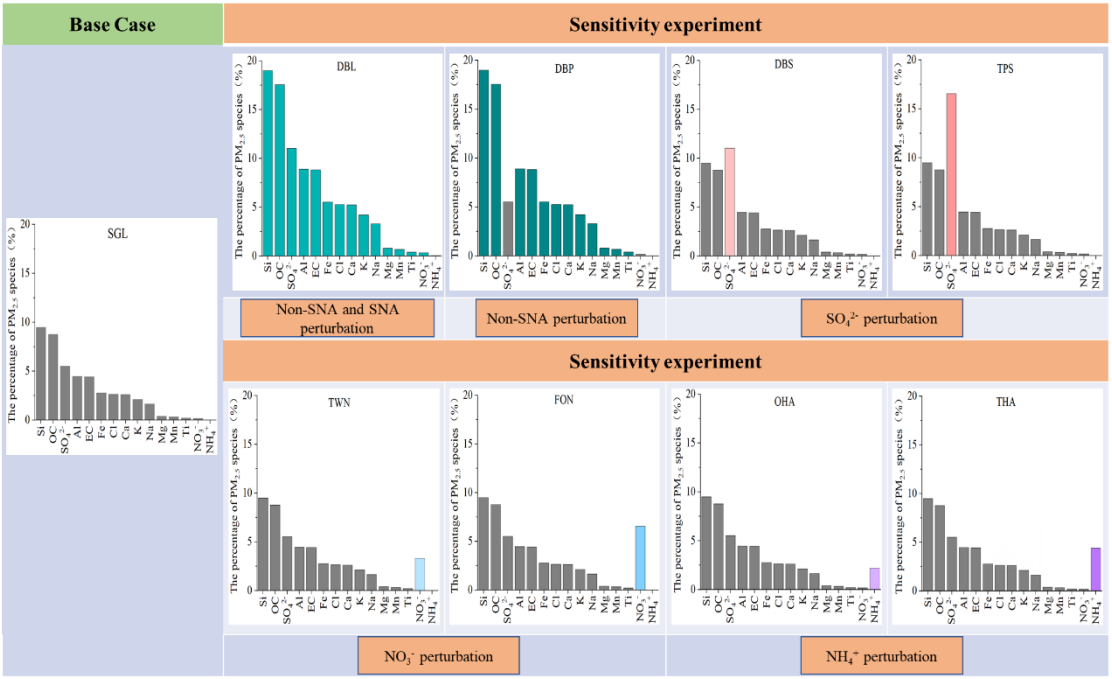

Fig. 4 The general roadmap of sensitivity tests (The histogram in each case were the speciation profile in CTMs; SNA represented SO_4^{2-}, NO_3^-, and NH_4^+, Non-SNA represented other components in $PM_{2.5}$).

Table 1 The content of sensitivity experiment cases

Experiment Cases	Description[3]
Case DBL: add perturbation to Non-SNA and SNA[1]	The percentage of all the listed components in the source profile of base case (SGL) were doubled, and the proportion of unlisted components (Other)[2] decreased to 9%.
Case DBP:	The percentages of non-SNA were doubled and SNA(SO_4^{2-},

add perturbation to Non-SNA	NO_3^-, NH_4^+) species stayed the same with that in SGL (the cumulative percentage of listed species was 85.3%), the proportion of unlisted components decreased to 14.7%.
Case DBS and TPS: add perturbation to SO_4^{2-}	The percentage of SO_4^{2-} was doubled (11%, DBS, represented Double Sulfate), tripled (16.5%, TPS, represented Triple Sulfate) and the other listed 14 species stayed the same with that in SGL (the cumulative percentage of listed species was 51% and 57%, respectively), the proportion of unlisted components decreased to 49% and 43%.
Case TWN and FON: add perturbation to NO_3^-	The NO_3^- content was raised up to 20 times (3.3%, TWN) and 40 times (6.6%, FON) of that in SGL (0.16%), the other 14 species stayed the same with SGL (the cumulative percentage of listed species was 48.6% and 51.9%, respectively), the proportion of unlisted components decreased to 51.4% and 48.1%.
Case OHA and THA: add perturbation to NH_4^+	The NH_4^+ content was raised up to 100 times (2.2%, OHA), 200 times (4.4%, THA) of that in SGL (0.02%), the other 14 species stayed the same with SGL (the cumulative percentage of listed species was 47.7% and 49.9%, respectively), the proportion of unlisted components decreased to 52.3% and 50.1%.

Note:

1. SNA represented SO_4^{2-}, NO_3^-, and NH_4^+, Non-SNA represented other components in $PM_{2.5}$.
2. The listed components contained Al, Ca, Cl, EC, Fe, K, Mg, Mn, Na, OC, Si, Ti, NH_4^+, NO_3^- and SO_4^{2-}, unlisted components were classified as Other.
3. The source profiles in all cases listed in the table were calculated based on the base case SGL. In the design of simulation cases, the reason why the disturbance amplitude of NH_4^+ and NO_3^- were significantly higher than that of other components such as SO_4^{2-} and Non-SNA, was because the percentages of NH_4^+ and NO_3^- in the base source profile (SGL, based on the chemical composition of code 000002.5 in the EPA Speciate_5.0_0 database) were very low, while the percentage of NH_4^+ and NO_3^- in SPAPPC exhibited in section 2.2 were orders of magnitude higher than those in SGL.

309 Given the large number and complex chemical composition of $PM_{2.5}$, it was
310 advisable to classify them reasonably before designing sensitivity experiments. The
311 Case DBL was to double the percentage of the listed 15 components mentioned in the
312 above base case(SGL) (the details are shown in Fig. 4 and Table 1). As the percentage
313 of these components increased, the proportion of unlisted components (represented by
314 "Other") decreased to 9% in order to meet the requirement that the total percentage of
315 all components is 100%. Then we compared the simulation results before (SGL case)

and after perturbation (DBL case) in species allocation of $PM_{2.5}$ sources.

In the case DBL, when the percentage of all the components except "other" were doubled in the source profile, the simulated concentrations of Al, Ca, Cl, EC, Fe, K, Mg, Mn, Na, OC, Si and Ti doubled as well, while the simulated concentration of NO_3 and SO_4^{2-} increased at about 3%, 10% and NH_4^+ decreased by 4%, respectively, although the simulated concentration of $PM_{2.5}$ was not obviously changed (Detailed simulation results were shown in Table S14). The simulation test results for SNA (SO_4^{2-}, NO_3^-, and NH_4^+) and Non-SNA were obviously different. Therefore, we divided the components in the source profile into two groups (Non-SNA and SNA) and designed a series of sensitivity tests listed in next section to further explore how species allocation of $PM_{2.5}$ in emission sources affect the simulation results. The sketch of sensitivity experiment design idea was shown in Figure S7.

4.1 Sensitivity tests design

Sensitivity tests were designed by changing the percentages of the target components and related components in the base case (SGL): add perturbation on each component of Non-SNA, on SO_4^{2-}, on NO_3^-, and on NH_4^+. The general roadmap of sensitivity tests was shown in Fig. 4, and the illustration of each case was summarized in Table 1. The basic rules must be followed: a) perturbation on the percentage of each component in source profile fell within the variation range of its measured value described in section 2.2. b) The sum of the percentage of listed Non-SNA, SNA and Other components in $PM_{2.5}$ source profile was 100%.

4.2 Sensitivity of simulated components to changes in source profile

We propose the sensitivity coefficient (δ) as evaluation index. The calculation formula is as follows:

$$\delta_{i,p} = \frac{\frac{C_{i\_case}}{C_{PM_{2.5}\_case}} \times 100\% - \frac{C_{i\_base}}{C_{PM_{2.5}\_base}} \times 100\%}{P_{p\_case} - P_{p\_base}} \quad (For\ DBL\ and\ DBP, p = i; For\ other\ cases,\ p = j) \qquad \text{..... (2)}$$

Wherein, $\delta_{i,p}$ is the sensitivity coefficient of component *i* relative to component p,

representing the change in simulated value of its content in ambient $PM_{2.5}$ corresponded to 1% perturbation in the source profiles. C_{i_case} is the simulated concentration of component i in each sensitivity experiment case, μg/m^3; C_{i_base} is the simulated concentration of components i in base case, μg/m^3; $C_{PM_{2.5}\_case}$ is the simulated concentration of $PM_{2.5}$ in each sensitivity experiment case, μg/m^3; $C_{PM_{2.5}\_base}$ is the simulated concentration of $PM_{2.5}$ in base case, μg/m^3; P_{p_case} is the percentage of component p in source profile of sensitivity experiment case, %; j is the perturbed component j in different source profile of sensitivity experiment cases; P_{p_base} is the percentage of component p in source profile of base case, %.

The positive value of δ means the simulated concentration of $PM_{2.5}$ component increases (decreases) with the increase (decrease) of perturbation on the percentage of components in source profile, negative δ is just the opposite. If the absolute value of δ is less than or equal to 0.1, the simulated component is considered to be insensitive to the corresponding variation of source profile; If the absolute value of δ falls between 0.1 and 0.4 (included), the simulated component is considered to be sensitive to the variation of source profile; If the absolute value of δ is larger than 0.4, the simulated component is very sensitive to the variation of source profile. The greater the absolute value of δ is, indicates the variation of source profile adopted in CMAQ has more obvious impact on the simulated results of $PM_{2.5}$ chemical components.

Fig.5 listed the sensitivity coefficients of simulated ambient $PM_{2.5}$ components to the perturbation of source profile under each test case. In case DBL (doubled the percentage of the listed components in the source profile of base case and decreased the proportion of unlisted other components to 9%), the sensitivity coefficient (δ) of NH_4^+ was negative, and the absolute value was high, indicating that the simulated proportion of NH_4^+ in ambient $PM_{2.5}$ decreased, and it was very sensitive to the variation of source profile. Conversely, the sensitivity coefficient of NO_3^- was close to 1, which illustrated that the simulated proportion of NO_3^- in ambient $PM_{2.5}$ increased proportionally with the change in source profile. The simulated SO_4^{2-} also showed a very sensitive property.

The simulated Non-SNA concentrations were doubled when compared to the base case (SGL).

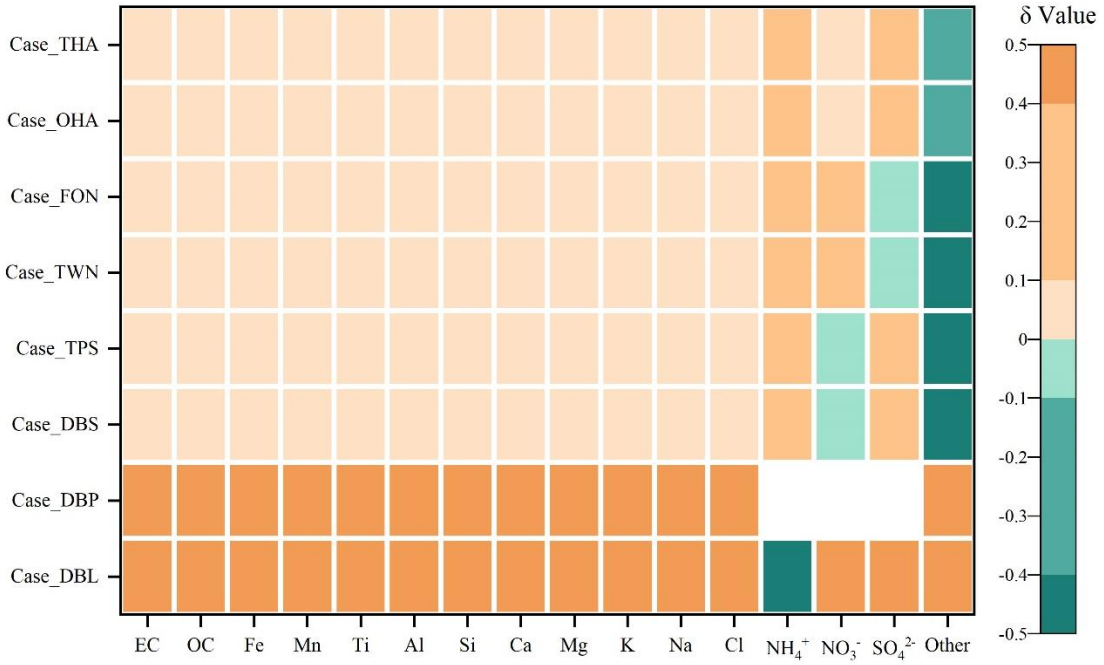

Fig. 5 The sensitivity coefficients (δ) of simulated components to the perturbation of adopted source profile in different cases. Note: Each small color box in the figure represented the sensitivity level (indicated by the legend on the right) of $PM_{2.5}$ components (the x-coordinate) in different cases (y-coordinate). The blank grids in DBP case indicated no perturbation to SNA in $PM_{2.5}$ source profile under this case.

In case DBP, when the percentages of listed Non-SNA (Al, Ca, Cl, EC, Fe, K, Mg, Mn, Na, OC, Si and Ti) in the source profile were doubled, the simulated proportions of Non-SNA in ambient $PM_{2.5}$ synchronous increased, and were very sensitive to the change in the adopted source profile with a sensitivity coefficient (δ) of 0.5. Interestingly, the simulated concentration of SNA in ambient $PM_{2.5}$ also changed although the SNA in source profile did not change, the concentration of NO_3^- and SO_4^{2-} increased by 2% and 3%, respectively, NH_4^+ decreased by 10% (Detail simulation results of each case were shown on Table S15~S21).

Under SO_4^{2-} perturbation cases (Case DBS and Case TPS), we found the simulated results of Non-SNA and NO_3^- had no obvious variation compared with the base case. Either in Case DBS or in Case TPS, the δ of Non-SNA and NO_3^- were between -0.1 to 0.1. But when the percentage of SO_4^{2-} was doubled in source profile (DBS), the

simulated concentration of NH_4^+ and SO_4^{2-} increased by 6% and 8%, respectively. In Case TPS (the percentage of SO_4^{2-} was tripled), the simulated concentration of NH_4^+ and SO_4^{2-} were increased by 11% and 16%, respectively. The δ of NH_4^+ and SO_4^{2-} were 0.12 and 0.36, sensitive toward to positive direction with the increase of SO_4^{2-} in the source profile.

In the situation of NO_3^- perturbation in source profile (Case TWN and Case FON), the simulated Non-SNA hardly change when compared to the base case, while changing patterns of simulated SNA were different. The simulation concentration of NH_4^+ increased by 2.6% and 5.4% compared with the base case, the simulated NO_3^- increased by 14% and 30%, the simulated SO_4^{2-} decreased slightly, even could be neglected in some observation sites. The simulated concentrations of Non-SNA and SO_4^{2-} were insensitive to the perturbation of NO_3^- in source profile; NH_4^+ was sensitive, and NO_3^- was very sensitive.

When we put perturbation on NH_4^+ in the source profile (Case OHA and Case THA), the simulation results of Non-SNA were almost not changed, the simulated concentration of SO_4^{2-}, NH_4^+, NO_3^- increased. The δ of SNA to the variation of NH_4^+ in the source profile were positive and $\delta_{SO_4^{2-},NH_4^+} > \delta_{NH_4^+,NH_4^+} > \delta_{NO_3^-,NH_4^+}$, SO_4^{2-} and NH_4^+ were sensitive to the NH_4^+ perturbation in the source profile, but NO_3^- was not so sensitive.

In general, the simulation results of components in ambient $PM_{2.5}$ were affected in one way or another by the change of source profiles adopted by CMAQ. Both of the simulated Non-SNA and SNA were very sensitive to the perturbation of Non-SNA in source profile. When the percentage of SNA changed in the source profile, simulated Non-SNA generally have little change, but the simulation results of SNA could change in different patterns: the simulated SO_4^{2-} was very sensitive and NH_4^+ was sensitive to the perturbation of SO_4^{2-} in source profile; simulated NO_3^- was very sensitive and NH_4^+ was sensitive to the perturbation of NO_3 in source profile$^-$; SO_4^{2-} and NH_4^+ were sensitive to the perturbation of NH_4^+ in source profile. The simulated component such as SO_4^{2-} was influenced not only by the change of SO_4^{2-} itself but also by other

components like some Non-SNA and NH_4^+ in the source profile. In other words, there was a linkage effect, variation of some components in the source profile would bring changes to the simulated results of other components.

5 How does the impact work?

The variation of species allocation in emission sources can directly affect the composition of aerosol system in CTMs. In CMAQv5.0.2, the aerosol thermodynamic equilibrium process is carried out according to ISORROPIA II, including a SO_4^{2-}-NO_3^--Cl^--NH_4^+-Na^+-K^+-Mg^{2+}-Ca^{2+}-H_2O system (Detailed equilibrium relations were shown in Table S22). Some assumptions have been made in the ISORROPIA model to simplify the simulation system (Fountoukis and Nenes, 2007): (1) Because the vapor pressure of sulfuric acid and metal salts (such as Na^+, Ca^{2+}, K^+, Mg^{2+}) are very low, it is assumed that all the sulfuric acid and metal salts in the system existed in the aerosol phase; (2) For ammonia in the system, it is preferred to have an irreversible reaction with sulfuric acid to produce ammonium sulfate. Only when there is still surplus NH_3 after the neutralization of H_2SO_4, can it have a reversible reaction with HNO_3 and HCl to produce NH_4NO_3 and NH_4Cl. (3) For sulfuric acid in the system, if there are metal ions (such as Ca^{2+}, Mg^{2+}, K^+, Na^+) in the system, sulfuric acid would react with metal ions to produce metal salts. Only in the case of insufficient sodium, sulfuric acid would react with ammonia. Based on these assumptions, the ISORROPIA model introduces the following three judgment parameters (R_1, R_2 and R_3) to determine the simulation subsystems, these parameters are calculated by the following formulas:

$$R_1 = \frac{\left[NH_4^+\right]+\left[Ca^{2+}\right]+\left[K^+\right]+\left[Mg^{2+}\right]+\left[Na^+\right]}{\left[SO_4^{2-}\right]} \quad (3)$$

$$R_2 = \frac{\left[Ca^{2+}\right]+\left[K^+\right]+\left[Mg^{2+}\right]+\left[Na^+\right]}{\left[SO_4^{2-}\right]} \quad (4)$$

$$R_3 = \frac{\left[Ca^{2+}\right]+\left[K^+\right]+\left[Mg^{2+}\right]}{\left[SO_4^{2-}\right]} \quad (5)$$

Where [X] denotes molar concentration of component ($mol \cdot m^{-3}$), R_1, R_2 and R_3

are termed as “total sulfate ratio”, “crustal species and sodium ratio” and “crustal species ratio” respectively; The number of species and equilibrium reactions are determined by the relative abundance of NH_3, Na, Ca, K, Mg, HNO_3, HCl, H_2SO_4, as well as the ambient relative humidity and temperature. Guide by the value of R_1, R_2 and R_3, 5 aerosol composition regimes in ISORROPIA are defined. (Detail rules are shown in Table S27 and solving procedure in Figure S8). R_1, R_2 and R_3 under each sensitivity test case were shown in Fig. 6. These components achieved thermodynamic equilibrium in the order of preference for more stable salts, obviously, the simulation processes of these components may influence each other.

5.1 General results

Our sensitivity experiment focuses on examining the impact of source profile changes on simulated $PM_{2.5}$ components. For given meteorological conditions, we analyze the sensitivity of simulated components to variations in the source chemical profile by comparing the simulation results between perturbed cases and base case.

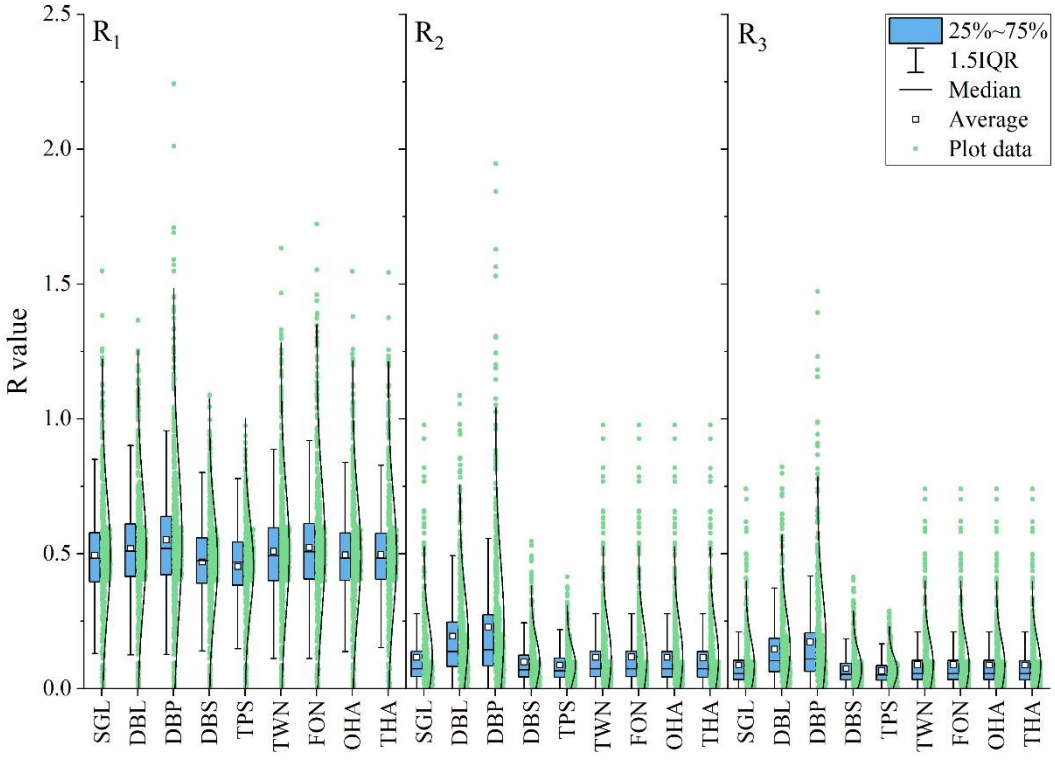

Fig. 6 R values’ distribution of among base case and different sensitivity test cases

In Non-SNA perturbation case, when the percentage of Non-SNA in source profile

doubled (Case DBP), meant there were more Na, K, Mg, Ca, Cl participated in aerosol chemistry, the model system needed more SO_4^{2-} and NO_3^- on the basis of charge balance and the thermodynamic equilibrium shifted to the direction of consuming Ca Mg, K and Na, which resulted in the increase of the simulated concentration of SO_4^{2-} and NO_3^-. Meanwhile, according to the rule of anions preferentially binding with nonvolatile cations in ISORROPIA, the increased cations Na^+, K^+, Mg^{2+}, Ca^{2+} directly leaded to the decrease of anions binding with NH_4^+, there were less reaction dose between SO_4^{2-} and NH_4^+ to form $(NH_4)_2SO_4$ or NH_4HSO_4, ultimately resulted in a decrease in simulated concentration of NH_4^+ compared with the base case. Because in this case more anions such as SO_4^{2-} were passively needed, according to the principle of chemical equilibrium mentioned above, the chemical conversion of SO_2 to SO_4^{2-} was promoted, the simulated secondary SO_4^{2-} increased, this could be proved by that the sensitivity coefficient δ of SO_2 in Case DBP was negative (shown in Fig. 7, details of other monitoring stations' results were shown Table S25).

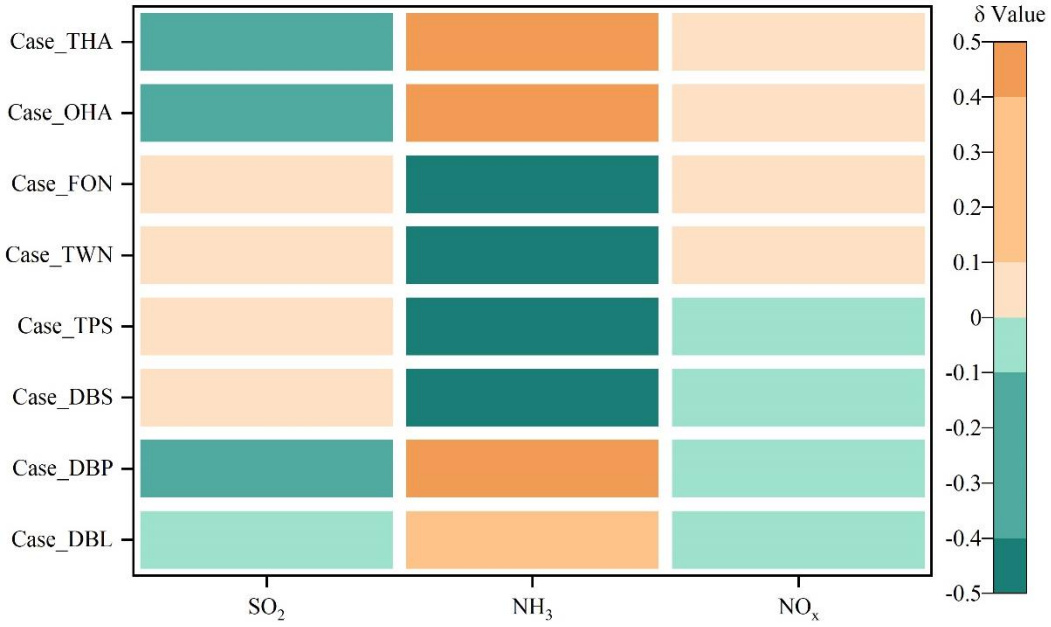

Fig.7 The sensitivity coefficients (δ) of simulated gas pollutants to the change of adopted source profile in different cases.

Similarly, with the increase of metal ions in the system to bond with anions, the number of anions which can bind to NH_4^+ decreased. The system needed less NH_4^+ and weakened the need for conversion from NH_3 to NH_4^+, the simulated NH_4^+ concentration

decreased while the δ of NH_3 was positive and very sensitive. Different trends of simulated concentration of gaseous pollutants mirrored the rules mentioned above from another aspect. The δ of SO_2 and NO_x was negative, NH_3 was positive. We could see the same phenomena in DBL case (Fig. 7). When the percentages of Non-SNA in source profile increased, they not only affected the simulated concentration of Non-SNA, but also the secondary SO_4^{2-}, NO_3^- and NH_4^+.

In SO_4^{2-} perturbation cases (Case DBS and TPS), as the percentage of SO_4^{2-} in source profile increased, for the chemical reactions of sulfate radical consuming (as shown in Table S22), the chemical equilibrium would move toward the products compared with the base case. While for the chemical reactions of sulfate radical formation (The equations were shown in Table S23), meant the product was added in, the chemical equilibrium would be pushed toward the reactants. The chemical reactions between SO_4^{2-} and NH_4^+ would shift to the direction of $(NH_4)_2SO_4$ or NH_4HSO_4 generation, we could see the simulated concentrations of NH_4^+ in DBS and TPS were both higher and NH_3 were lower than those in the base case (SGL). In addition, when more SO_4^{2-} was added in the system, the conversion of SO_2 to SO_4^{2-} was affected in some level and consumed less SO_2 than the base case, simulated SO_2 showed insensitive but positive trend (Fig.7). And the potential solid phase species in ISORROPIA II under DBS and TPS cases (shown in Table S27) were mainly consisted of sulfate salts, so the simulated concentration of NO_3^- did not change apparently.

As the percentage of NO_3^- in source profile increased (Case FON and TWN), the associated chemical equilibrium shifted towards the consumption of NO_3^-, such as $NH_4^+ + NO_3^- \rightarrow NH_4NO_3$, which would also consume more NH_4^+ and form more ammonium salt, finally consumed more NH_3 because of $NH_3(gas) + H_2O(aq) \rightarrow NH_4^+(aq) + OH^-(aq)$. The simulation results also manifested that the concentration of NH_4^+ increased while that of NH_3 decreased. Based on the assumption of ISORROPIA, the cations like Na^+, K^+, Mg^{2+}, Ca^{2+} and NH_4^+ preferentially to react with SO_4^{2-}, only if there were cations left after neutralized SO_4^{2-}, could they react with NO_3^- to form salts, so the simulated concentration of SO_4^{2-} was not obviously changed. Accordingly, the

simulated concentration of NO_x and SO_2 almost unchanged (The δ of NO_x and SO_2 displayed insensitive).

In the cases of NH_4^+ perturbation (Case OHA and THA), when the percentage of NH_4^+ in source profile increased, the related chemical equilibrium shifted towards the direction of NH_4^+ consumption, such as in $2NH_4^+ + SO_4^{2-} \rightarrow (NH_4)_2SO_4$ or $NH_4^+ + H^+$, $SO_4^{2-} \rightarrow NH_4HSO_4$, more SO_4^{2-} was consumed at the same time, which further promoted the conversion of SO_2 to SO_4^{2-}. The increased NH_4^+ in OHA and THA also would inhibit the conversion of NH_3 to NH_4^+ compared with the base case. This, in turn appeared as the increase of the simulated secondary SO_4^{2-} and NH_3, and the decrease of the simulated SO_2.

5.2 Results from stratified analysis

For each case, the distribution of R values was related to meteorological conditions (as shown in Fig. 6). To illustrate the role of meteorological conditions in the mechanism of how source profile affected the simulated $PM_{2.5}$ components, stratified analysis was used. The hourly simulation result of temperature and humidity (affecting ISORROPIA solving procedure), wind field (affecting flux in and flux out for each grid) were incorporate into K-means clustering. When the number of clusters was equal to or greater than 4, there was a significant inflection point between data points and their assigned cluster centroids (Figure S9). Hence, 4 patterns of meteorological conditions were selected to the subsequent analysis.

For pattern I, II, III and IV, as shown in Fig. 8, the rule similar to the general result was observed. From a global view, the subdivisional (category-specific) sensitivity of simulated $PM_{2.5}$ components to source chemical profile under different patterns are similar; From a local perspective, their sensitivity levels are slightly different; For example, in pattern II, the simulated NH_4^+ was very sensitive to the perturbation of SO_4^{2-}; While in pattern I, III and VI was sensitive, but it remained the major component that underwent change (These results were also shown in Table S28 of supplementary material).

When we perturb source profile, some species/reactants increase (or reduce) in the

system, the chemical equilibrium shift to the direction of consuming more (or less) reactants, as shown in Figure S10. Under different patterns of meteorological conditions (determining the values of R), the influence pathways of chemical source profile changes on the simulated $PM_{2.5}$ components have the same laws with general results.

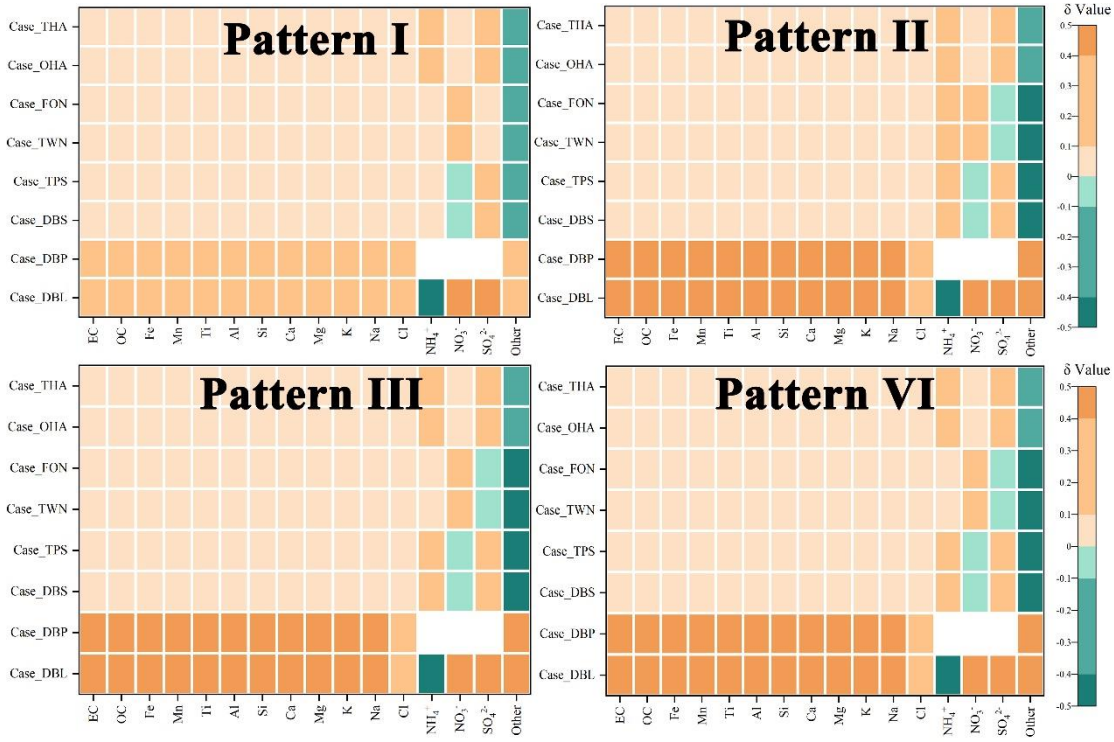

Fig. 8 The sensitivity coefficients (δ) under different hierarchical patterns

In summary, the effects of source profile variation on the simulation results of different components were linked. When the percentages of Non-SNA, SO_4^{2-}, NO_3^- and NH_4^+ in the source profile changed, they not only affected the simulated concentration of themselves, but also affected the simulation results of some other components. Both the simulation results of primary components and secondary components were affected by the change of source profile, the secondary SO_4^{2-} and NH_4^+ were affected more than the secondary NO_3^-.

6 Conclusions

The influence of source profile variation on the simulated $PM_{2.5}$ components cannot be ignored, as simulation results of some components are sensitive to the adopted source profile in CTMs, e.g., both the simulated Non-SNA and SNA are

sensitive to the perturbation of Non-SNA in source profile, the simulated SO_4^{2-} and NH_4^+ are sensitive to the perturbation of SO_4^{2-}, simulated NO_3^- and NH_4^+ are sensitive to the perturbation of NO_3^-, SO_4^{2-} and NH_4^+ are sensitive to the perturbation of NH_4^+. These influences are not only specific to an individual component, but also can be transmitted and linked among components. The influence path is connected to chemical mechanisms in the model since the variation of species allocation in emission sources directly affect the thermodynamic equilibrium system (ISORROPIA II, SO_4^{2-}-NO_3^--Cl^--NH_4^+-Na^+-K^+-Mg^{2+}-Ca^{2+}-H_2O system).

It is generally believed that changes in source profile would have an impact on the simulation result of primary $PM_{2.5}$, but interestingly, the simulation of secondary components could be affected as well. We found the perturbation of $PM_{2.5}$ source profile caused the variation of simulation results of gaseous pollutants by influencing related chemical reactions like gas-phase chemistry of SO_2, NO_x and NH_3. Overall, the emission source profile used in CTMs is one of the important factors affecting the simulation results of $PM_{2.5}$ chemical components. Additionally, organic species are one of the most important components in $PM_{2.5}$ and gain much more attention on human health. While the number of organic species in source profile is relatively scarce which brings a challenge for simulation test designing, the influence of source profile on the simulation results of organic species is not taken into account in this study.

With the change of fuel and raw materials, the development of production technology and the innovation of pollution treatment technology in recent years, some components have changed significantly in source profiles. Given the important role of air quality simulation in decision making for pollution control and health risk assessment, the representativeness and timeliness of the source profile should be considered.

Our study tentatively discussed the influence mechanism of $PM_{2.5}$ emission source profiles on the simulation results of components in CTMs. The size distribution, mixing state, aging and solubility for different aerosol components might have something to do with source profile, how much the influence of source profile changes on the simulation

of these physical and chemical process, is deserved to do in the future.

Data availability

The input datasets for WRF simulation are available at https://rda.ucar.edu/datasets/ds351.0/index.html (The National Center for Atmospheric Research (NCAR)). The Multi-resolution Emission Inventory for China (MEICv1.3) is available at http://meicmodel.org/?page_id=135. The $PM_{2.5}$ emission source profiles from database of Source Profiles of Air Pollution (SPAP) (http://www.nkspap.com:9091/, Nankai university), SPECIATE database (https://www.epa.gov/air-emissions-modeling/speciate, U.S. Environmental Protection Agency's (EPA)), Mendeley data repository (https://doi.org/10.17632/x8dfshjt9j.2, Bi et al., 2019). Tutorial guide for accessing Database of Source Profiles of Air Pollution (SPAP), input and output data repository (https://zenodo.org/record/7865675).

Code availability

The source code for CMAQ version 5.0.2 is available at https://github.com/USEPA/CMAQ/tree/5.0.2 (last access: April 2014) (https://doi.org/10.5281/zenodo.1079898, US EPA Office of Research and Development, 2018). The source code for WRF version 3.7.1 is available at https://www2.mmm.ucar.edu/wrf/src/WRFV3.7.1.TAR.gz.

Author contributions

Zhongwei Luo: Data curation and collection, writing–original draft. Yan Han: Modeling, writing–original draft. Kun Hua: Data collection. Yufen Zhang: Supervision–Review & editing. Jianhui Wu: Supervision in source profile. Xiaohui Bi: Supervision in source profile. Qili Dai: Resources. Baoshuang Liu: Resources. Yang Chen: Modification and editing. Xin Long: Supervision in modeling. Yinchang Feng: Supervision–Review & editing.

Competing interests

The authors declare that they have no known competing financial interests or personal relationships that could have appeared to influence the work reported in this paper.

Disclaimer. Publisher's note

Copernicus Publications remains neutral with regard to jurisdictional claims in published maps and institutional affiliations.

Acknowledgements

We would like to thank the National Natural Science Foundation of China (grant number 42177465) for providing funding for the project. We are grateful for the Inventory Spatial Allocate Tool (ISAT) provided by Kun Wang from Department of Air Pollution Control, Institute of Urban Safety and Environmental Science, Beijing Academy of Science and Technology. We thank three anonymous referees, Astrid Kerkweg (Executive Editor) and Klaus Klingmüller (Top Editor) for the time and effort spent in reviewing the manuscript.

Financial support

This study was financially supported by the National Natural Science Foundation of China (grant number 42177465).

Reference

Appel, K. W., Poulio, G. A., Simon, H., Sarwar, G., Pye, H. O. T., Napelenok, S. L., Akhtar, F., Roselle, S. J.: Evaluation of dust and trace metal estimates from the Community Multiscale Air Quality (CMAQ) model version 5.0, Geosci. Model Dev., 6, 883-899, https://doi.org/10.5194/gmd-6-883-2013, 2013.

Bi, X., Dai, Q., Wu, J., Zhang, Q., Zhang, W., Luo, R., Cheng, Y., Zhang, J., Wang, L., Yu, Z., Zhang, Y., Tian, Y., Feng, Y.: Characteristics of the main primary source profiles of particulate matter across China from 1987 to 2017, Atmos. Chem. Phys., 19, 3223-3243, https://doi.org/10.5194/acp-19-3223-2019, 2019.

Cao, J., Qiu, X., Gao, J., Wang, F., Wang, J., Wu, J., Peng, L.: Significant decrease in SO_2 emission and enhanced atmospheric oxidation trigger changes in sulfate formation pathways in China during 2008–2016, J. Clean. Prod., 326, 129396, https://doi.org/10.1016/j.jclepro.2021.129396,

2021.
Chapel Hill, N.: Operational Guidance for the Community Multiscale Air Quality (CMAQ) Modeling System Version 5.0, https://www.airqualitymodeling.org/index.php/CMAQ_version_5.0_(February_2010_release)_OGD#Aerosol_Module, last access: February 2012.
Chen, Z., Chen, D., Zhao, C., Kwan, M., Cai, J., Zhuang, Y., Zhao, B., Wang, X., Chen, B., Yang, J., Li, R., He, B., Gao, B., Wang, K., Xu, B.: Influence of meteorological conditions on $PM_{2.5}$ concentrations across China: A review of methodology and mechanism, Environ. Int., 139, 105558, https://doi.org/10.1016/j.envint.2020.105558, 2020.
Cheng, N. L., Meng, F., Wang, J. K., Chen, Y. B., Wei, X., Han, H.: Numerical simulation of the spatial distribution and deposition of $PM_{2.5}$ in East China coastal area in 2010 (In Chinese), Journ. Safety Environ., 15, 305-310, https://doi.org/10.13637/j.issn.1009-6094.2015.06.063, 2015.
Eder, B. K., Yu, S. C.: A performance evaluation of the 2004 release of Models-3 CMAQ, Atmos. Environ., 40, 4811-4824, http://doi.org/10.1007/978-0-387-68854-1_57, 2006.
Foley, K. M., Roselle, S. J., Appel, K. W., Bhave, P. V., Pleim, J., Otte, T., Mathur, R., Sarwar, G., Young, J. O., Gilliam, R.: Incremental testing of the community multiscale air quality (CMAQ) modeling system version 4.7, Geosci. Model Dev., 3, 205-226, https://doi.org/10.5194/gmd-3-205-2010, 2010.
Fountoukis, C., Nenes, A.: ISORROPIA II: a computationally efficient thermodynamic equilibrium model for K^+–Ca^{2+}–Mg^{2+}–NH_4^+–Na^+–SO_4^{2-}–NO_3^-–Cl^-–H_2O aerosols, Atmos. Chem. Phys., 7, 4639-4659, https://doi.org/10.5194/acp-7-4639-2007, 2007.
Fu, X., Wang, S., Zhao, B., Xing, J., Cheng, Z., Liu, H., Hao, J.: Emission inventory of primary pollutants and chemical speciation in 2010 for the Yangtze River Delta region, China, Atmos. Environ., 70, 39-50, https://doi.org/10.1016/j.atmosenv.2012.12.034, 2013.
Fu, X., Wang, S. X., Chang, X., Cai, S., Xing, J., Hao, J. M.: Modeling analysis of secondary inorganic aerosols over China: pollution characteristics, and meteorological and dust impacts, Sci. Rep., 6, 35992, https://doi.org/10.1038/srep35992, 2016.
Gao, S., Zhang, S., Che, X., Ma, Y., Chen, X., Duan, Y., Fu, Q., Wang, S., Zhou, B., Wei, C., Jiao, Z.: New understanding of source profiles: Example of the coating industry, J. Clean. Prod., 357, 132025, https://doi.org/10.1016/j.jclepro.2022.132025, 2022.
Guo, R., Yang, J., Liu, Z.: Influence of heat treatment conditions on release of chlorine from Datong coal, J. Anal. Appl. Pyrol., 71, 179-186, https://doi.org/10.1016/S0165-2370(03)00086-X, 2004.
Guo, Y. Y., Gao, X., Zhu, T. Y., Luo, L., Zheng, Y.: Chemical profiles of PM emitted from the iron and steel industry in northern China, Atmos. Environ., 150, 187-197, https://doi.org/10.1016/j.atmosenv.2016.11.055, 2017.
Guo, Z., Hao, Y., Tian, H., Bai, X., Wu, B., Liu, S., Luo, L., Liu, W., Zhao, S., Lin, S., Lv, Y., Yang, J., Xiao, Y.: Field measurements on emission characteristics, chemical profiles, and emission factors of size-segregated PM from cement plants in China, Sci. Total Environ., 151822, https://doi.org/10.1016/j.scitotenv.2021.151822, 2021.
Han, Y., Xu, H., Bi, X. H., Lin, F. M., Li, J., Zhang, Y. F., Feng, Y. C.: The effect of atmospheric particulates on the rainwater chemistry in the Yangtze River Delta, China, J. Air Waste Manage., 69, 1452-1466, https://doi.org/10.1080/10962247.2019.1674750, 2019.
Hopke, P. K., Dai, Q., Li, L., Feng, Y.: Global review of recent source apportionments for airborne

particulate matter, Sci. Total Environ., 740, 140091, https://doi.org/10.1016/j.scitotenv.2020.140091, 2020.
Hopke, P. K., Feng, Y. C., Dai, Q.: Source apportionment of particle number concentrations: A global review, Sci. Total Environ., 819, 153104, https://doi.org/10.1016/j.scitotenv.2022.153104, 2022.
Hsu, Y., Divita, F., Dorn, J.: SPECIATE 5.0 - Speciation Database Development Documentation, Final Report, M. MENETREZ, Abt Associates Inc./Office of Research and Development/U.S. Environmental Protection Agency Research Triangle Park, NC27711, https://www.epa.gov/sites/default/files/2019-07/documents/speciate_5.0.pdf, 2019.
Huang, C. H., Hu, J. L., Xue, T., Xu, H., Wang, M.: High-Resolution Spatiotemporal Modeling for Ambient $PM_{2.5}$ Exposure Assessment in China from 2013 to 2019, Environ. Sci. Technol., 55, 2152-2162, https://doi.org/10.1021/acs.est.0c05815, 2021.
Huang, Z. J., Zheng, J. Y., Qu, J. M., Zhong, Z. M., Wu, Y. Q., Shao, M.: A Feasible Methodological Framework for Uncertainty Analysis and Diagnosis of Atmospheric Chemical Transport Models, Environ. Sci. Technol., 53, 3110-3118, https://doi.org/10.1021/acs.est.8b06326, 2019.
Ji, Z., Gan, M., Fan, X., Chen, X., Li, Q., Lv, W., Tian, Y., Zhou, Y., Jiang, T.: Characteristics of $PM_{2.5}$ from iron ore sintering process: Influences of raw materials and controlling methods, J. Clean. Prod., 148, 12-22, https://doi.org/10.1016/j.jclepro.2017.01.103, 2017.
Li, J., Wu, Y., Ren, L., Wang, W., Tao, J., Gao, Y., Li, G., Yang, X., Han, Z., Zhang, R.: Variation in $PM_{2.5}$ sources in central North China Plain during 2017–2019: Response to mitigation strategies, J. Environ. Manage., 28, 112370, https://doi.org/10.1016/j.jenvman.2021.112370, 2021.
Li, M., Hu, M., Du, B., Guo, Q., Tan, T., Zheng, J., Huang, X., He, L., Wu, Z., Guo, S.: Temporal and spatial distribution of $PM_{2.5}$ chemical composition in a coastal city of Southeast China, Sci. Total Environ., 605-606, 337-346, https://doi.org/10.1016/j.scitotenv.2017.03.260, 2017a.
Li, M., Liu, H., Geng, G., Hong, C., Liu, F., Song, Y., Tong, D., Zheng, B., Cui, H., Man, H., Zhang, Q., He, K.: Anthropogenic emission inventories in China: a review, Natl. Sci. Rev., 4, 834-866, https://doi.org/10.1093/nsr/nwy044, 2017b.
Li, X., He, K., Li, C., Yang, F., Zhao, Q., Ma, Y., Chen, Y., Ouyang, W., Chen, G.: $PM_{2.5}$ mass, chemical composition, and light extinction before and during the 2008 Beijing Olympics, J. Geophys. Res., 118, 12158-12167, https://doi.org/10.1002/2013JD020106, 2013.
Liang, F., Xiao, Q., Yang, X., Liu, F., Li, J., Lu, X., Liu, Y., Gu, D.: The 17-y spatiotemporal trend of $PM_{2.5}$ and its mortality burden in China, Proc. Natl. Acad. Sci., 117, 25601-25608, https://doi.org/10.1073/pnas.1919641117, 2020.
Lv, L., Wei, P., Li, J., Hu, J.: Application of machine learning algorithms to improve numerical simulation prediction of $PM_{2.5}$ and chemical components, Atmos. Pollut. Res., 12, 101211, 10.1016/j.apr.2021.101211, 2021.
NBS (National Bureau of Stastistics of China): China Statistical Yearbook 2021, http://www.stats.gov.cn/tjsj/ndsj/2021/indexch.htm, last access: 2022.
Peterson, G., Hogrefe, C., Corrigan, A., Neas, L., Mathur, R., Rappold, A.: Impact of Reductions in Emissions from Major Source Sectors on Fine Particulate Matter–Related Cardiovascular Mortality, Environ, Health Persp., 128, 017005, https://doi.org/10.1289/EHP5692, 2020.
Qi, H., Cui, C., Zhao, T., Bai, Y., Liu, L.: Numerical simulation on the characteristics of $PM_{2.5}$ heavy pollution and the influence of weather system in Hubei Province in winter 2015 (In Chinese),

Meteorological monthly, 45, 1113-1122, https://doi.org/10.7519/j.issn.1000-0526.2019.08.008, 2019.
Seinfeld, J. H., Pandis, S. N.: Atmospheric Chemistry and Physics, from air pollution to climate change. John Wiley & Sons, Inc., Hoboken, New Jersey.47-61, ISBN9781119221166, 2006
Sha, T., Ma, X., Jia, H., Tian, R., Chang, Y., Cao, F., Zhang, Y.: Aerosol chemical component: Simulations with WRF-Chem and comparison with observations in Nanjing, Atmos. Environ., 218, 1-14, https://doi.org/10.1016/j.atmosenv.2019.116982, 2019.
Shi, W., Liu, C., Norback, D., Deng, Q., Huang, C., Qian, H., Zhang, X., Sundell, J., Zhang, Y., Li, B., Kan, H., Zhao, Z.: Effects of fine particulate matter and its constituents on childhood pneumonia: a cross-sectional study in six Chinese cities, Lancet, 392, S79, https://doi.org/10.1016/S0140-6736(18)32708-9, 2018.
Shi, Z., Li, J., Huang, L., Wang, P., Wu, L., Ying, Q., Zhang, H., Lu, L., Liu, X., Liao, H., Hu, J.: Source apportionment of fine particulate matter in China in 2013 using a source-oriented chemical transport model, Sci. Total Environ., 601-602, 1476-1487, https://doi.org/10.1016/j.scitotenv.2017.06.019, 2017.
Song, S. Y., Wang, Y. S., Wang, Y. L., Wang, T., Tan, H. Z.: The characteristics of particulate matter and optical properties of Brown carbon in air lean condition related to residential coal combustion, Powder Technol., 379, 505-514, https://doi.org/10.1016/j.powtec.2020.10.082, 2021.
Tang, X. Y., Zhang, Y. H., Shao, M.: Atmosphere Environment Chemistry, Second ed (In Chinese). . Higher Education Press, Beijing, China.268-329, ISBN978-7-04-019361-9, 2006
Wang, C., Zheng, J., Du, J., Wang, G., Klemes, J., Wang, B., Liao, Q., Liang, Y.: Weather condition-based hybrid models for multiple air pollutants forecasting and minimisation, J. Clean. Prod., 352, 131610, https://doi.org/10.1016/j.jclepro.2022.131610, 2022.
Wang, D., Hu, J., Xu, Y., Lv, D., Xie, X., Kleeman, M., Xing, J., Zhang, H., Ying, Q.: Source contributions to primary and secondary inorganic particulate matter during a severe wintertime $PM_{2.5}$ pollution episode in Xi'an, China, Atmos. Environ., 97, 182-194, https://doi.org/10.1016/j.atmosenv.2014.08.020, 2014.
Weagle, C., Sinder, G., Li, C. C., Donkelaar, A., S, P., Bissonnette, P., Burke, I., Jackson, J., Latimer, R., Stone, E., Abboud, I., Akoshile, C., Anh, N., Brook, J., Cohen, A., Dong, J., Gibson, M., Griffith, D., He, K., Holben, B., Kahn, R., Keller, C., Kim, J., Lagrosas, N., Lestari, P., Khian, Y., Liu, Y., Marais, E., Martins, J., Misra, A., Muliane, U., Pratiwi, R., Quel, E., Salam, A., Segey, L., Tripathi, S., Wang, C., Zhang, Q., Brauer, M., Rudich, Y., Martin, R.: Global Sources of Fine Particulate Matter: Interpretation of $PM_{2.5}$ Chemical Composition Observed by SPARTAN using a Global Chemical Transport Model, Environ. Sci. Technol., 52, 11670-11681, https://doi.org/10.1021/acs.est.8b01658, 2018.
Wongphatarakul, V., Friedlander, S. K., Pinto, J. P.: A Comparative Study of $PM_{2.5}$ Ambient Aerosol Chemical Databases, Environ. Sci. Technol., 32, 3926-3934, https://doi.org/10.1021/es9800582, 1998.
Wu, B., Bai, X., Liu, W., Zhu, C., Hao, Y., Lin, S., Liu, S., Luo, L., Liu, X., Zhao, S., Hao, J., Tian, H.: Variation characteristics of final size-segregated PM emissions from ultralow emission coal-fired power plants in China, Environ. Pollut., 259, 113886, https://doi.org/10.1016/j.envpol.2019.113886, 2020.
Wu, D., Zheng, H., Li, Q., Jin, L., Lyu, R., Ding, X., Huo, Y., Zhao, B., Jiang, J., Chen, J., Li, X.,

Wang, S.: Toxic potency-adjusted control of air pollution for solid fuel combustion, Nat. Energy, 7, 194-202, https://doi.org/10.1038/s41560-021-00951-1, 2022.
Wu, Z. X., Hu, T. F., Hu, W., Shao, L. Y., Sun, Y. Z., Xue, F. L., Niu, H. Y.: Evolution in physicochemical properties of fine particles emitted from residential coal combustion based on chamber experiment, Gondwana Res., https://doi.org/10.1016/j.gr.2021.10.017, 2021.
Xia, Z. Q., Fan, X. L., Huang, Z. J., Liu, Y. C., Yin, X. H., Ye, X., Zheng, J. Y.: Comparison of Domestic and Foreign $PM_{2.5}$ Source Profiles and Influence on Air Quality Simulation (In Chinese), Res. Environ. Sci., 30, 359-367, https://doi.org/10.13198/j.issn.1001-6929.2017.01.55, 2017.
Yang, F., Tan, J., Zhao, Q., Du, Z., He, K., Ma, Y., Duan, F., Chen, G., Zhao, Q.: Characteristics of $PM_{2.5}$ speciation in representative megacities and across China, Atmos. Chem. Phys., 11, 1025-1051, https://doi.org/10.5194/acpd-11-1025-2011, 2011.
Ying, Q., Feng, M., Song, D. L., Wu, L., Hu, J., Zhang, H., Kleeman, M., Li, X.: Improve regional distribution and source apportionment of $PM_{2.5}$ trace elements in China using inventory-observation constrained emission factors, Sci. Total Environ., 624, 355-365, https://doi.org/10.1016/j.scitotenv.2017.12.138, 2018.
Yu, S. C., Mathur, R., Pleim, J., Wong, D., Gilliam, R., Alapaty, K., Zhao, C., Liu, X.: Aerosol indirect effect on the grid-scale clouds in the two-way coupled WRF-CMAQ: model description, development, evaluation and regional analysis, Atmos. Chem. Phy., 14, 11247-11285, http://10.5194/acp-14-11247-2014, 2014.
Yu, Z. C., Jang, M., Kim, S., Bae, C., Koo, B., Beardsley, R., Park, J., Chang, L., Lee, H., Lim, Y., Cho, J.: Simulating the Impact of Long-Range-Transported Asian Mineral Dust on the Formation of Sulfate and Nitrate during the KORUS-AQ Campaign, Earth Space Chem., 4, 1039-1049, https://doi.org/10.1021/acsearthspacechem.0c00074, 2020.
Zhang, J., Wu, J., Lv, R., Song, D., Huang, F., Zhang, Y., Feng, Y.: Influence of Typical Desulfurization Process on Flue Gas Particulate Matter of Coal-fired Boilers (In Chinese), Environ. Sci., 41, 4455-4461, https://doi.org/10.13227/j.hjkx.202003193, 2020.
Zhang, Q., Xue, D., Wang, S., Wang, L., Wang, J., Ma, Y., Liu, X.: Analysis on the evolution of $PM_{2.5}$ heavy air pollution process in Qingdao (In Chinese), China Environ. Sci., 37, 3623-3635, https://doi.org/10.3969/j.issn.1000-6923.2017.10.003, 2017.
Zhang, S. P., Xing, J., Sarwar, G., Ge, Y. L., He, H., Duan, F., Zhao, Y., He, K., Zhu, L., Chu, B.: Parameterization of heterogeneous reaction of SO_2 to sulfate on dust with coexistence of NH_3 and NO_2 under different humidity conditions, Atmos. Environ., 208, 133-140, https://doi.org/10.1016/j.atmosenv.2019.04.004, 2019.
Zheng, B., Tong, D., Li, M., Liu, F., Hong, C., Geng, G., Li, H., Li, X., Peng, L., Qi, J., Yan, L., Zhang, Y., Zhao, H., Zheng, Y., He, K., Zhang, Q.: Trends in China's anthropogenic emissions since 2010 as the consequence of clean air actions, Atmos. Chem. Phys., 18, 14095-14111, https://doi.org/10.5194/acp-18-14095-2018, 2018.
Zheng, B., Zhang, Q., Zhang, Y., He, K. B., Wang, K., Zheng, G. J., Duan, F. K., Ma, Y. L., Kimoto, T.: Heterogeneous chemistry: a mechanism missing in current models to explain secondary inorganic aerosol formation during the January 2013 haze episode in North China, Atmos. Chem. Phys., 15, 2031–2049, 10.5194/acp-15-2031-2015, 2015.
Zheng, H., Song, S., Sarwar, G., Gen, M., Wang, S., Ding, D., Chang, X., Zhang, S., Xing, J., Sun, Y. L., Ji, D., Chan, C. K., Gao, J., Mcelory, M.: Contribution of Particulate Nitrate Photolysis

817 to Heterogeneous Sulfate Formation for Winter Haze in China, Environ. Sci. Technol. Lett., 7,
818 632-638, https://doi.org/10.1021/acs.estlett.0c00368, 2020.
819 Zhou, L., Chen, X., Tian, X.: The impact of fine particulate matter ($PM_{2.5}$) on China's agricultural
820 production from 2001 to 2010, J. Clean. Prod., 178, 133-141,
821 https://doi.org/10.1016/j.jclepro.2017.12.204, 2018.
822